Available online at www.sciencedirect.com
SCIENCE DIRECT®
Journal of APPLIED MATHEMATICS AND MECHANICS
ELSEVIER
www.elsevier.com/locate/jappmathmech
Journal of Applied Mathematics and Mechanics 69 (2005) 680–692

THE OPTIMUM SHAPES OF BODIES MOVING IN A MEDIUM TAKING FRICTION INTO ACCOUNT†

G. Ye. YAKUNINA
Moscow
email: galina_yakunina@mail.ru

(*Received* 16 *December* 2004)

Within the limits of the model of local interaction of a body and a medium, the special features of the design of optimum three-dimensional bodies are investigated taking friction into account. It is assumed that the pressure on the body surface is described by a two-term formula which is quadratic in the velocity and has constant terms representing the strength of the medium. Three models of the friction are used to represent the shear stresses: constant friction, friction proportional to the pressure, and mixed friction. A comparative analysis is carried out of solutions of problems of optimizing the body shape with respect to drag and with respect to penetration depth, obtained in the class of three-dimensional configurations for the different models of the friction. It is shown that, if the base area of the body is given, the optimum shapes for all the friction models are those in which the normal at each point makes a constant optimum angle with the direction of motion. This angle is independent of the base area and is determined by the velocity of motion and the parameters of the model, which depend on the characteristics of the medium. The influence of the parameters of the model on the optimum shapes is demonstrated and, for each model, formulae are derived relating the velocity of motion and the characteristics of the medium with the optimum angle.

It is well known that when a body is moving in dense media, such as soil and metal, the friction forces exert a considerable influence on the characteristics of the motion of the body [1–5] and may even cause it to break [2]. The characteristics of the motion of the body may be improved and the risk of breakage reduced if one uses body shapes that, at the first stage, have the minimum drag or guarantee the maximum penetration depth at a certain initial velocity of motion.

The search for the optimum shapes must be carried out taking friction into account. However, owing to the great variety of properties of media, which often depend on the velocity and loading conditions, it is difficult to give exact quantitative estimates of the influence of friction, and approximate models are therefore constructed to allow for this [1–5]. Local interaction models,in which it is assumed that each element of the body surface interacts with the medium independently of other parts of the body, have been widely used to describe the forces acting on the surface of a body moving at high velocity in media. Thus, when investigating the motion of a body in dense media, one most often uses a two-term local interaction model [4–11], in which the pressure on the body surface is described by a formula that is quadratic in the velocity and has constant terms characterizing the strength of the medium; shear stresses are represented using one of two models: constant friction or Coulomb friction. In the constant friction model it is assumed that the shear stresses are equal to their maximum value and constant over the whole body surface. Such a model is frequently used to describe shear stresses on the surface of a body moving at high velocities in media of low or medium strength, such as gases or soils [4, 5]. The Coulomb friction model, in which the shear stresses are assumed to be proportional to the pressure, is most often used to describe the forces acting on a body moving in highly resistant media, such as concrete and metal [3, 7, 10, 11].

The use of a two-term local interaction model with constant, velocity-independent parameters enables the drag and penetration depth of the body to be represented as a functional [4, 7–14] that depends explicitly on the body shape. This enables the search for optimum shapes using the methods of the

†*Prikl. Mat. Mekh.* Vol. 69, No. 5, pp. 759–774, 2005.
0021–8928/$—see front matter.
doi: 10.1016/j.jappmathmech.2005.09.003

calculus of variations, and it has been proved [8, 12–14] that, in the class of three-dimensional (3D) shapes with a given base area of the body, minimum drag and maximum penetration depth are achieved by bodies with the property that the normal to their surface at each point makes a constant optimum angle with the motion direction. This angle is independent of the base area of the body and is determined by the characteristics of the medium and the velocity of the body motion in terms of the constants occurring in the drag law. In the general case, the optimum angles for bodies of minimum drag and bodies with maximum penetration depth are different, but the technique for constructing these bodies is the same [12–14].

Friction influences the shape of the optimum bodies, and it has been shown [13, 14] that, without allowing for friction in the two-term local interaction model, the optimum 3D bodies are constructed from pieces of surfaces whose normals are perpendicular to the direction of motion. For a given non-zero base area, the optimum shapes in that case will be those with infinite lateral surface area. Such shapes are of no practical use, and therefore, the solution of problems of the optimization of bodies must allow for friction, but the choice of friction model must be justified specifically as it applies to a specific medium.

A generalization of the models just considered to the case of a body moving in dense media is the mixed friction model proposed for soils in [1]. In that model the shear stresses are calculated by Coulomb's friction law if they do not exceed the yield point of the material of the medium in shear, and equal to the yield point otherwise. As a result, in any body shape, there may be parts of the surface on which shear stresses are evaluated using different friction laws.

The problem of a body of minimum drag using a mixed friction model in the two-term local interaction model has been solved for solids of revolution [9]. In the class of 3D shapes, the special features of the solution of this problem have not been analysed. The problem of a body with maximum penetration depth has never been considered in the case of a mixed friction model.

Remark. After this paper had gone to print, K. A. Koneva and N. A. Ostapenko published a paper entitled "Three-dimensional bodies of least drag moving in dense media under conditions of a mixed friction model" (*Vestnik Mosk. Univ., Ser. 1, Matematika, Mekhanika*, 2004, 6, 34–39). In that paper, using the approach of [12–14], the solution of the problem of a body of minimum drag in the mixed-friction model is analysed. However, the results of the computations are given there for a medium referred to as "soil," but whose strength characteristics are lower by almost two orders of magnitude than those of soils; consequently, the conclusions drawn in that paper on the basis of those computation cannot be used to investigate real dense media.

Below, using a two-term local interaction model in the class of 3D configurations, a comparative analysis is carried out of solutions of the problems of a body of minimum drag and a body with maximum penetration depth, for three friction models: constant friction, Coulomb friction and mixed friction. The differences between these solutions are demonstrated and the influence of the model parameters on the optimum body shapes are investigated.

1. THE MODEL OF THE BODY–MEDIUM INTERACTION

The force that a medium exerts on a rigid non-deformable body moving in it may be written in the form

$$\mathbf{F} = \iint_S [\sigma_n \mathbf{n} + \sigma_\tau \boldsymbol{\tau}] dS \tag{1.1}$$

where σ_n and σ_τ are the normal and shear stresses on the body surface, $\mathbf{n}$ and $\boldsymbol{\tau}$ are the unit vectors of the inward normal and the tangent to a surface element; the integration is performed over the surface S of contact of the body with the medium.

We shall assume that each element of the surface S interacts with the medium independently of other parts of the body, and that the action of the forces on the surface may be described by a local interaction model [4–11]. To represent the stresses in the local interaction model, we will use two-term formulae containing dynamical and constant terms

$$\sigma_n = A_1 U^2 (\mathbf{u} \cdot \mathbf{n})^2 + B_1, \quad \sigma_\tau = A_2 U^2 (\mathbf{u} \cdot \mathbf{n})^2 + B_2 \tag{1.2}$$

where U is the velocity of the body, $\mathbf{u}$ is the unit vector of the velocity, and the coefficients A_i and B_i ($i = 1, 2$) are the parameters of the model, determined by the characteristics of the medium. With certain

assumptions, the first expression of (1.2) describes the pressure on the surface of the body moving in a gas [4] and in dense media like soils and metals [5–10]. The term B_1 in that case characterizes the resistance of the medium to deformation, and the coefficient A_1 is of the order of magnitude of the density of the medium. For specific media, the values of A_1 and B_1 are determined either by solving model problems [5, 6] or by experiment [15, 16]. Thus, for clay media, according to the solution obtained for an incompressible elastoplastic medium [6], one can take

$$A_1 = 3\rho_0/2, \quad B_1 = 4\tau_s(1 + \ln(\mu/\tau_s))/3 \tag{1.3}$$

where ρ_0 is the density of the medium, μ is the shear modulus and is τ_s is the yield point of the material of the medium for shear; all these are constant and independent of the velocity.

In the local interaction model, the vector τ is coplanar with $\mathbf{u}$ and $\mathbf{n}$:

$$\boldsymbol{\tau} = [[\mathbf{u} \times \mathbf{n}] \times \mathbf{n}]/|[\mathbf{u} \times \mathbf{n}]| \tag{1.4}$$

The shear stresses σ_τ will be represented using three models: constant friction, Coulomb friction and a mixed friction model. The constant friction model is frequently chosen to represent σ_τ on the body surface when the body is moving at high velocity in media of low and average strength, such as gas and soils [4, 5], when it is assumed that the shear stresses have reached their maximum values and are equal to the yield point τ_s, which is constant over the entire body surface: $\sigma_\tau = \tau_s$. Then

$$A_2 = 0, \quad B_2 = \tau_s \tag{1.5}$$

The Coulomb model is most frequently used to describe the forces acting on the body when it is moving in strong media, such as concrete and metal [3, 7, 10, 11]. Within the framework of this model, shear stresses are assumed to be proportional to the pressure: $\sigma_\tau = \mu_0\sigma_n$, where μ_0 is the constant coefficient of friction, and in that case,

$$A_2 = \mu_0 A_1, \quad B_2 = \mu_0 B_1 \tag{1.6}$$

A generalization of these models to the case of a body moving in dense media is the mixed friction model, in which the shear stresses are evaluated by Coulomb's law of friction if they do not exceed τ_s and equal to τ_s otherwise:

$$\sigma_\tau = \begin{cases} \mu_0\sigma_n, & \text{if} \quad \mu_0\sigma_n \le \tau_s \\ \tau_s, & \text{if} \quad \mu_0\sigma_n \ge \tau_s \end{cases} \tag{1.7}$$

In model (1.7), the body surface, whatever its shape, may contain sections on which the shear stresses are computed by different friction laws. However, analysis of conditions (1.7) using expressions (1.2) shows that this possible only when the velocity of the body and the parameters of the medium satisfy the inequality

$$0 < b < \lambda; \quad b = C/\mu_0 - 1, \quad C = \tau_s/B_1, \quad \lambda = A_1U^2/B_1 \tag{1.8}$$

If inequality (1.8) is violated on the entire body surface, a uniform friction law must be used to evaluate σ_τ. Thus, if $b \le 0$, the second condition of (1.7) is always true and σ_τ must be evaluated using the constant friction model (1.5); but if $b \ge \lambda$, the first inequality of (1.7) is always true and σ_τ must be evaluated using the Coulomb model (1.6).

The quantity C depends only on the characteristics of the medium; the coefficient μ_0 depends on the friction properties of the interacting materials of the medium and body, and the number λ depends on the properties of the medium and the velocity of the body. Estimates of C and μ_0 may be obtained by analysing their approximate values in real media [4–6, 10].

Thus, using expression (1.3) for B_1 and taking into account that $\mu/\tau_s \gg 1$ for most media, we deduce that $C \in$ [0.09, to 0.29] in the range of μ/τ_s values from 5 to 10^3. Analogous estimates for C may be obtained in other approximations [4, 5, 10]. For the coefficient μ_0 one most frequently uses the range $\mu_0 \in$ [0.01, 0.1] for a metallic impactor moving in a metallic obstruction [10] and the range $\mu_0 \in$ [0.1, 0.2] for a metallic impactor moving in soil.

Thus, the non-dimensional quantities C and μ_0 may be assumed to satisfy the following constraints, which will be used below in our derivation of results

$$0.1 \le C \le 0.3, \quad 0.01 \le \mu_0 \le 0.2 \tag{1.9}$$

The use of model (1.2) for any of the ways considered above for evaluating σ_τ enables us to represent the forces **F** (1.1) and its components as explicit functions of the body shape. This property of the two-term local interaction model (1.2) for specific friction laws has been used before [4, 7–9, 11–14] when solving a great many problems of body shape optimization. However, for the mixed friction model (1.7) a solution of the problem of the body of maximum penetration depth has not been found before.

Below, based on conclusions reached in [8, 12–14] for optimum shapes within the framework of a local interaction model of generalized form, we present a comparative analysis of solutions of the problem of the body of minimum drag and the body with maximum penetration depth in the class of 3D configurations for the two-term model (1.2) and friction models (1.5)–(1.7).

2. THREE-DIMENSIONAL MINIMUM DRAG SHAPES

Suppose a body is moving in the direction opposite to that of the vector **x**: $\mathbf{x} = -\mathbf{u}$. Let S be entire lateral surface of the body and assume that there

$$\alpha = (\mathbf{n} \cdot \mathbf{x}) \geq 0 \tag{2.1}$$

Using expressions (1.2) and (1.4) to evaluate the force **F** (1.1) and noting that $(\tau \cdot \mathbf{x}) = \gamma$, $\gamma = (1-\alpha^2)^{1/2}$, we can write the drag of the body in the form

$$D = (\mathbf{F} \cdot \mathbf{x}) = B_1 \iint_S f(\alpha)\alpha dS; \quad f(\alpha) = 1 + \lambda\alpha^2 + B\gamma(k\lambda\alpha^2 + 1)/\alpha, \quad B = B_2/B_1 \tag{2.2}$$

where $k = 0$ for model (1.5) and $k = 1$ for model (1.6). At a fixed velocity, λ is constant. The coefficients B and k are also constant and independent of α if the stresses σ_τ (1.2) are evaluated in the constant friction model (1.5):

$$B = C, \quad k = 0 \tag{2.3}$$

or in the Coulomb friction model (1.6):

$$B = \mu_0, \quad k = 1 \tag{2.4}$$

In these cases expression (2.2) for $f(\alpha)$ may be written as in the form

$$f(\alpha) = \begin{cases} f_1(\alpha) \text{ for the constant friction model} \\ f_2(\alpha) \text{ for the Coulomb friction model} \end{cases} \tag{2.5}$$

$$f_1(\alpha) = 1 + \lambda\alpha^2 + \gamma C/\alpha, \quad f_2(\alpha) = (1 + \lambda\alpha^2)(1 + \gamma\mu_0/\alpha)$$

In the mixed friction model (1.7), B and k depend on α, and if

$$\alpha \leq \alpha_k, \quad \alpha_k = (b/\lambda)^{1/2} \tag{2.6}$$

then expressions (2.4) are used for B and k and $f(\alpha) = f_2(\alpha)$. If $\alpha > \alpha_k$, expressions (2.3) are taken for B and k and $f(\alpha) = f_1(\alpha)$. If $f(\alpha)$ is considered as a function of the real variable α in the interval [0, 1], then $f(\alpha)$ is a positive, continuous function: $f_1(\alpha_k) = f_2(\alpha_k)$ and, taking expressions (2.5) into account, we have

$$f(\alpha) = \inf(f_1(\alpha), f_2(\alpha)) \tag{2.7}$$

Independently of the ways considered above for evaluating σ_τ, model (1.2) is a special case of writing the stresses within the framework of the local interaction model. In a local interaction model of generalized form it has been proved [12–14] that in the class of 3D configurations, for non-separating flow around the body and given base area S_b of the body, minimum drag is obtained for bodies at each point of whose surface the following condition holds

$$\alpha = \alpha^* = \text{const} \tag{2.8}$$

where α^* is the value of α at which the function $f(\alpha)$ has a minimum in the interval [0, 1]. This value is independent of S_b and is determined by the parameters λ, k and B occurring in expression (2.2) for $f(\alpha)$.

It has been shown [12–14] that for given S_b values and constraints imposed on the length and transverse dimensions of the body, one can construct an infinite set of bodies satisfying condition (2.8). These bodies have been called "absolutely optimal," since they all have the same drag, which is the least possible for the given base area.

A minimum of the function $f(\alpha)$ is sought among its local and boundary extrema. The values of $\alpha = \alpha_m$ for local minima satisfy the conditions $f'(\alpha_m) = 0$ and $f''(\alpha_m) > 0$. Using expression (2.2) for $f(\alpha)$, we can rewrite the equation $f'(\alpha) = 0$ in the form

$$2\lambda\alpha^3\gamma + kB\lambda\alpha^2(\gamma^2 - \alpha^2) - B = 0 \tag{2.9}$$

A boundary minimum is possible only when $\alpha = 1$, since if $\alpha \to 0$, then $f(\alpha) \to \infty$. As a result, the required point α^* is such that

$$f(\alpha^*) = \inf(f(\alpha_m), f(1)), \quad f(1) = 1 + \lambda \tag{2.10}$$

The value of $f(1)$ is the same for models (1.5) and (1.6), and the local minima of the function $f(\alpha)$ must be compared with that value. If $f(1) < f(\alpha_m)$, then $\alpha^* = 1$ and an absolutely optimal body is an end plane of given area.

For friction models (1.5) and (1.6), the solutions of Eq. (2.9) are determined by the parameters B and λ. In the thin-body approximation, when

$$\alpha^2 \ll 1 \tag{2.11}$$

these solutions in model (1.5) depend on the value of one parameter E, $E = B/\lambda$:

$$\alpha_m = (E/2)^{1/3} \tag{2.12}$$

For model (1.6), the approximate solutions of Eq. (2.9) may also be represented by expression (2.12) but, as follows from Cardano's formulae for the roots of cubic equations, that can only be done subject to the additional condition $\lambda\mu_0^2/27 \ll 1$. This condition is true under the constraints (1.9) and $\lambda \leq 50$; in that case, consequently, in both friction models (1.5) and (1.6), expression (2.12) can be used for α_m in the approximation (2.11).

Note that as B increases the quantities α_m also increase, but as λ increases they decrease. It can be shown that an increase in α_m implies an increase in $f(\alpha_m)$. The increase in $f(\alpha_m)$ when $\alpha^* = \alpha_m$ is bounded by $f(1)$, which is reached when $B = B^*$ and $\alpha_m = \alpha_m^* : f(\alpha_m^*) = f(1)$. Using Eq. (2.9), we can write the expressions

$$B^* = \lambda/(2\sqrt{1 + k\lambda}), \quad \alpha_m^* = 1/\sqrt{1 + k\lambda}$$

Curves 1 and 2 in Fig. 1 are graphs of B^* as a function of λ, constructed for models (1.5) and (1.6), respectively. Note that if $\lambda > 1$, then $B^* > 0.3$, so that under conditions (1.9) $B < B^*$. When $B < B^*$ we have $\alpha^* = \alpha_m < \alpha_m^* \leq 1/\sqrt{2}$. Using relations (2.1) and (2.8), one can verify that in that case the angle between the outward normal to the surface of an absolutely optimal body and the direction of motion always exceeds 45°. If $B \geq B^*$, then $\alpha^* = 1$ and the angle in question is 0°.

If $B \leq 0.3$ and $\lambda \in [1, 50]$, formula (2.12) gives a good approximation to the exact solutions of Eq. (2.9), and it can be shown that in that case, in friction models (1.5) and (1.6), the drag of a body constructed with $\alpha = \alpha_m$ (2.12) will increase compared with that of an absolutely optimal body by less than 3%.

The solutions of Eq. (2.9) we analysed above for models (1.5) and (1.6). In the mixed model (1.7), it follows from relations (2.7) and (2.10) that the minimum of $f(\alpha)$ should be sought among the minima of functions (2.5), and it depends on μ_0, C and λ.

The domain of μ_0 and λ values that satisfy inequality (1.8), for which friction model (1.7) is used, is shown for $C = 0.1$ in Fig. 2; it lies between the dash-dot curve emanating from the point with coordinates $(\mu_0, \lambda) = (0.1, 0)$ and the line $\mu_0 = 0.1$. Within that domain in Fig. 2 lies curve 1, representing the relations between the parameters μ_0 and λ when $C = 0.1$ for which

$$\inf(f_1(\alpha)) = \inf(f_2(\alpha)) \tag{2.13}$$

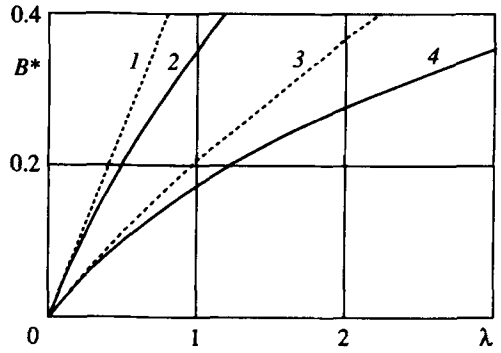

Fig. 1

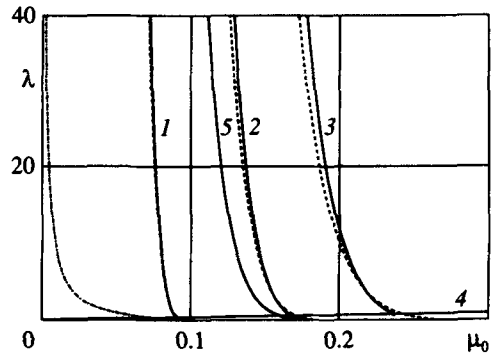

Fig. 2

If the point with coordinates (μ_0, λ) lies below curve *1*, the value of α^* (2.8) used to construct an absolutely optimal body is evaluated in friction model (1.6); otherwise model (1.5) is used. As C increases the domain of μ_0 and λ values for which α^* is evaluated by model (1.6) expands, lying in Fig. 2 to the left of curves 2 and 3, which were constructed for $C = 0.2$ and $C = 0.3$, respectively.

Also shown in Fig. 2 is curve 4, constructed for μ_0 and λ for which $f(\alpha_m) = f(1)$. If the point (μ_0, λ) lies outside curve 4, then $\alpha^* = \alpha_m$, otherwise $\alpha^* = 1$.

The solid curves 1–3 in Fig. 2 were constructed for μ_0 and λ values for which condition (2.13) is satisfied. In the approximation (2.11), local minima of the functions (2.5) are reached when $\alpha = \alpha_m$ (2.12), and in that case condition (2.13) is true if $\lambda = \lambda_k$, where

$$\lambda_k = 27((C/\mu_0)^{2/3} - 1)^3/(2\mu_0^2) \tag{2.14}$$

Figure 2 presents λ_k as a function of μ_0 – the dashed curves 1, 2 and 3, constructed for $C = 0.1$, 0.2 and 0.3, respectively. It can be seen that these curves are good approximations to the exact values of μ_0 and λ, which satisfy condition (2.13) without assuming that the body is thin.

As a result, the quantities $\alpha^* = \alpha_m$ in approximation (2.11) are found from the conditions

$$\alpha^* = \begin{cases} \alpha_1, & \text{if} \quad \lambda \geq \lambda_k \\ \alpha_2, & \text{if} \quad \lambda \leq \lambda_k \end{cases} \tag{2.15}$$

where

$$\alpha_1 = (C/(2\lambda))^{1/3}, \quad \alpha_2 = (\mu_0/(2\lambda))^{1/3} \tag{2.16}$$

The drag of an absolutely optimal body is less than the drag of any body with the same base area. For $C = 0.2$ and $\mu_0 = 0.15$, the solid curves 1, 2 and 3 in Fig. 3 represent the quantities ΔD, $\Delta D = (D(\alpha)/D(\alpha^*) - 1) \times 100$ for $\lambda = 1$, 5 and 50, respectively, showing by how many percent the drag $D(\alpha^*)$ of an absolutely optimal body in model (1.7) is less than the drag $D(\alpha)$ of cones constructed for

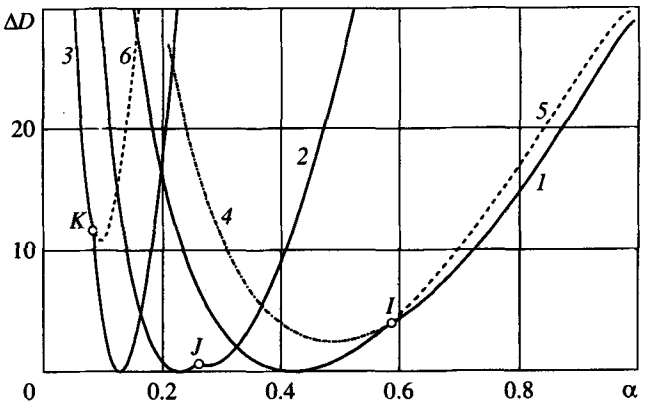

Fig. 3

different α and equivalent to the absolutely optimal body in length and base area. Using relations (2.2), one obtains $\Delta D = (\Delta f - 1) \times 100$, where $\Delta f = f(\alpha)/f(\alpha^*)$, and so curves 1–3 in Fig. 3 may be used to investigate the behaviour of the function $f(\alpha)$ over the interval [0, 1]. Curves 1, 2 and 3 have break points I, J and K, respectively, whose abscissae correspond to $\alpha = \alpha_k$ where, according to formulae (2.5)–(2.7), the graphs of the functions f_1 and f_2 intersect and the expressions for $f(\alpha)$ are changed. Curves 4 and 5 in Fig. 3, for $\lambda = 1$, represent the values of ΔD_1 and ΔD_2, respectively, where $\Delta D_i = (f_i(\alpha)/f(\alpha^*) - 1) \times 100$, $i = 1, 2$. It can be shown by analysing the relative positions of curves *1*, *4* and *5* how the graphs of the function f_1 and f_2 intersect for $\lambda = 1$. Curve 6 in Fig. 3, for $\lambda = 50$, $C = 0.2$ and $\mu_0 = 0.15$, represent the values of ΔD_2, and it can be shown that if the friction model (1.6) is used with these parameters, the optimal body obtained within the limits of that model will have a drag higher by 5% than that of the absolutely optimal body when the mixed friction model is used.

Thus, within the limits of the two-term local interaction model (1.2), we have carried out a comparative analysis of the solutions of the problem of a 3D shape of minimum drag provided by friction models (1.5)–(1.7). We have shown that, for a given base area of the body, in the mixed friction model (1.7), as in models (1.5) and (1.6), the optimum shape is made up of pieces of surfaces satisfying condition (2.8), in which α^* is found in terms of the parameters μ_0, C and λ. Unlike the optimum shape of solid of revolution [9], which may contain parts in which σ_τ is evaluated using different friction laws, the values of σ_τ on a surface of optimal 3D configuration are evaluated using uniform friction law (1.5) or (1.6). In the thin-body approximation (2.11), the relation between $\alpha^* = \alpha_m$ and the characteristics of the medium for friction models (1.5) and (1.6) is given by formula (2.12), while for the mixed friction model (1.7) it is given by formulae (2.14)–(2.16); for $\lambda \in [1, 50]$ and conditions (1.9) these formulae yield good approximations to the exact α^* values.

3. THREE-DIMENSIONAL SHAPES OF MAXIMUM PENETRATION DEPTH

Using expression (2.2) for the drag D of the body, we can write the equation of motion of a body mass m in the form

$$mdU/dt = -D, \quad D = A_1U^2D_1 + B_1D_2 \tag{3.1}$$

where

$$D_i = \iint_S g_i(\alpha)\alpha dS, \quad i = 1, 2; \quad g_1(\alpha) = \alpha^2\left(1 + kB\frac{\gamma}{\alpha}\right), \quad g_2(\alpha) = 1 + B\frac{\gamma}{\alpha} \tag{3.2}$$

Taking into consideration that $dH = Udt$, where H is the length of the body's trajectory, and also that

$$dU/dt = 1/2dU^2/dH$$

we can rewrite Eq. (3.1) for the variables H and λ, obtaining the following expression for the complete length H_0 of the body's trajectory

$$H_0 = \frac{m}{2A_1}\int_0^{\lambda_0}\frac{d\lambda}{\lambda D_1 + D_2}, \quad \lambda_0 = \frac{A_1 U_0^2}{B_1} \tag{3.3}$$

where U_0 is the initial velocity of the body.

If the functionals D_1 and D_2 are independent of λ, then

$$H_0 = \frac{m}{2A_1 D_1}\ln\left(1 + \lambda_0\frac{D_1}{D_2}\right) \tag{3.4}$$

For dense media, H_0 is the penetration depth of the body. Formula (3.4) may be used if D_1 and D_2 are constant and the parameters k and B occurring in (3.2) do not depend on U. This is true for friction models (1.5) and (1.6), with k and B as in (2.3) or (2.4).

It has been proved [8] that in the class of 3D shapes of given mass m and base area S_b, the maximum penetration depth H_0 (3.4) is attained by bodies in which, as in the case of minimum drag bodies, condition (2.8) holds at each point of the surface.

If $\alpha = \text{const}$

$$H_0 = M_0 h(\alpha), \quad M_0 = \frac{m\lambda_0}{2S_b A_1} = \text{const}$$
$$h(\alpha) = \frac{\ln(1+q)}{q(1 + B\gamma/\alpha)}, \quad q = \lambda_0\alpha^2\frac{\alpha + kB\gamma}{\alpha + B\gamma} \tag{3.5}$$

where the expression for $h(\alpha)$ has been derived from formulae (3.2) and (3.4).

For shapes of maximum penetration depth, α^* (2.8) is the argument α at which the function $h(\alpha)$ reaches a maximum in the interval [0, 1]. The value of α^* is independent of m and S_b, being determined by the parameters λ_0, k and B.

The maximum of the function $h(\alpha)$ is sought among its local and boundary extrema. The values of α_m at which $h(\alpha)$ attains a local maximum satisfy the $h'(\alpha_m) = 0$ and $h''(\alpha_m) < 0$. A boundary maximum of the function $h(\alpha)$ is only possible at $\alpha = 1$, since if $\alpha \to 0$, then $h(\alpha) \to 0$. Hence the required α^* is such that

$$h(\alpha^*) = \sup(h(\alpha_m), h(1)), \quad h(1) = \ln(1 + \lambda_0)/\lambda_0 \tag{3.6}$$

The quantity $h(1)$ is the same for models (1.5) and (1.6), and it must be compared with the local maxima of $h(\alpha)$. If $h(1) > h(\alpha_m)$, then $\alpha^* = 1$ and the body of maximum penetration depth is an end plane of given area.

The equation $h'(\alpha) = 0$ may be written as

$$2\lambda_0\alpha^3\gamma + kB\lambda_0\alpha^2(\gamma^2 - \alpha^2) - QB = 0, \quad Q = q^2/((q+1)\ln(q+1) - q) \tag{3.7}$$

Unlike Eq. (2.9), which was written for the extrema of $f(\alpha)$, Eq. (3.7) involves a function $Q = Q(q)$. If $q < 1$, we have an approximation for Q

$$Q = 2/(1 - q/3)$$

but if $q/3 \ll 1$, then $Q = 2$. Since $q \le \lambda_0\alpha^2$, this is true when

$$\alpha^2 \ll 3/\lambda_0 \tag{3.8}$$

If condition (3.8) holds and the thin-body approximation (2.11) is used for both friction models (1.5) and (1.6), then the solution of Eq. (3.7), like that of Eq. (2.9), is determined by the value of the parameter E; it is

$$\alpha_m = E^{1/3}, \quad E = B/\lambda_0 \tag{3.9}$$

For model (1.6), it is legitimate to write the solution in the form (3.9) if $\lambda_0\mu_0^2/54 \ll 1$, which is true under the constraints (1.9) and $\lambda_0 \leq 50$.

For fixed λ_0, if $B \to 0$, then $\alpha_m \to 0$, and it can be shown that $h(\alpha_m) \to 1$. Since $h(1) = \ln(1 + \lambda_0)/\lambda_0 < 1$, it follows that there is always a B^* such that, for $B < B^*$, we have $h(\alpha_m) > h(1)$, and consequently, for these B values, $\alpha^* = \alpha_m$. At the same time, if λ_0 is fixed and B is increased, then α_m will increase and $h(\alpha_m)$ will decrease. The increase in α_m is bounded by the value of α_m^* obtained for $B = B^*$: $h(\alpha_m^*) = h(1)$. It can be shown that, just as for minimum drag bodies, $\alpha_m^* \leq 1/\sqrt{2}$. Consequently, for $B < B^*$ we have $\alpha^* = \alpha_m < 1/\sqrt{2}$, and the angle between the outward normal to the surface of the optimum body and the direction of motion will always exceed 45°. For $B \geq B^*$ we have $\alpha^* = 1$, and the angle is 0°.

It should be mentioned that an abrupt change in the type of solution when the friction parameter reaches a certain value has been observed in the numerical solution of the problem of a slid of revolution with maximum penetration depth within the limits of model (1.6) [7]. This result, however, was perceived as undesirable [7] and interpreted as a transition to a minimum of the depth functional. It was shown above that the change in the type of solution when $B \geq B^*$ is natural, and it means that the maximum of the depth functional, previously a local extremum, has become a boundary extremum.

Curves 3 and 4 in Fig. 1 show B^* as a function of λ_0 for friction models (1.5) and (1.6), respectively. It can be shown that when $\lambda_0 > 2$ and constraints (1.9) hold, then $B^* > B$ and consequently in that case $\alpha^* = \alpha_m$.

The solution (3.9) was obtained in the approximation (2.11), subject to condition (3.8), which for large λ_0 is not always rigorously true for α_m. However, it can be shown that for both friction models, if $\lambda_0 \in [2, 50]$ and constraints (1.9) hold, then formula (3.9) gives a good approximation to the exact values of α_m and the penetration depth of bodies constructed with $\alpha = \alpha_m$ (3.9) is less than the maximum by at most 0.5%.

The results of a comparison of the penetration depth of bodies of minimum drag with the maximum penetration depth found for the same parameters as the minimum drag have shown that for $\lambda_0 \in [2, 50]$, if constraints (1.9) holds, the penetration depth of bodies constructed with $\alpha = \alpha_m$ (2.12) is less than the maximum by at most 3%. This conclusion is important for practical application of the results obtained, since it can be shown by an analysis of formulae (2.12) and (3.9) that an error of even a factor of two in the value of the parameter B is admissible if the relation $\alpha = \alpha_m$ (3.9) is used in the design of bodies. Then, if $\lambda_0 \in [2, 50]$ and constraints (1.9) hold, the penetration depth of the bodies thus designed will differ only slightly from the maximum.

The solutions of the problem of a body of maximum penetration depth were analysed above for friction models (1.5) and (1.6), with the penetration depth H_0 (3.3) expressed as a functional (3.4). In the case of the mixed friction model (1.7), there is no formula analogous to (3.4) for H_0, since in that case the parameters k and B in formulae (3.2) for D_1 and D_2 depend on λ and α. For a body of arbitrary shape, the values of k and B may differ in different parts of the body, and even in one part of the body they may change as λ is reduced from λ_0 to zero.

However, this does not exclude the possibility of using methods of the calculus of variations to maximize H_0 (3.3). At known values of m, S_b and λ_0, the penetration depth H_0 (3.3) is uniquely defined by the body shape. Consequently, in that case too H_0 may be considered as a functional, dependent on the body area S.

Suppose the surface S is defined in a cylindrical system of coordinates (x, r, θ) by the equation $x = \chi(r, \theta)$, where χ is a single-valued function of the points of the body base, whose contour is described by the equation $r = R(\theta)$. Then $\alpha dS = dS_b = rdrd\theta$, and formulae (3.2) may be rewritten in the form

$$D_i = \frac{1}{2}\int_0^{2\pi} d\theta \int_0^{R^2(\theta)} g_i(\alpha)dr^2, \quad i = 1, 2; \quad \int_0^{2\pi} R^2(\theta)d\theta = 2S_b \tag{3.10}$$

Note that the functions $\alpha(r, \theta)$ and $R(\theta)$ define the surface S and are independent of one another. The problem of constructing the shape of a 3D body of maximum penetration depth may be formulated as follows: among all piecewise-smooth functions $\alpha(r, \theta)$ and $R(\theta)$ that satisfy condition (2.1) and the last condition of (3.10), it is required to find those that make the functional H_0 (3.3) a maximum.

The Lagrange function for the functional (3.3) may be written in the form

$$L = H_0(\alpha, R) + \xi_0 \int_0^{2\pi} R^2(\theta)d\theta \tag{3.11}$$

where ξ_0 is a constant factor. Euler's equations for the functions $\alpha(r, \theta)$ and $R(\theta)$ of the extremal surface are found from the condition $\delta L = 0$, which, in view of formulae (3.3) and (3.11), may be written in the form

$$-\frac{m}{2A_1}\int_0^{\lambda_0}\frac{\lambda\delta D_1 + \delta D_2}{(\lambda D_1 + D_2)^2}d\lambda + \xi_0\int_0^{2\pi}\delta R^2 d\theta = 0 \tag{3.12}$$

where, in accordance with relations (3.2) and (3.10)

$$\delta D_i = \frac{1}{2}\int_0^{2\pi}d\theta\int_0^{R^2(\theta)}(g_i'(\alpha)\delta\alpha)dr^2 + \frac{1}{2}\int_0^{2\pi}(g_i(\alpha_f)\delta R^2)d\theta, \quad i = 1, 2$$
$$\alpha_f = \alpha(R(\theta), \theta); \quad g_1'(\alpha) = 2\alpha + kB\frac{\gamma^2 - \alpha^2}{\gamma}, \quad g_2'(\alpha) = -\frac{B}{\alpha^2\gamma} \tag{3.13}$$

Since the quantities λ_0, D_1, D_2 and ξ_0 are the same on the entire surface of the body, while $\delta\alpha$ and δR^2 are independent, it can be shown, using (3.13), that Eq. (3.12) will only hold when the function $\alpha(r, \theta)$ satisfies the conditions

$$\int_0^{\lambda_0}\frac{\lambda g_1'(\alpha) + g_2'(\alpha)}{(\lambda D_1 + D_2)^2}d\lambda = 0 \tag{3.14}$$

$$\int_0^{\lambda_0}\frac{\lambda g_1(\alpha_f) + g_2(\alpha_f)}{(\lambda D_1 + D_2)^2}d\lambda - \frac{4A_1}{m}\xi_0 = 0 \tag{3.15}$$

Equation (3.14) must hold at each point of the extremal surface of the body, and it involves no dependence of α on r and θ. The required function α is determined by the parameters λ_0, μ_0 and C, which are the same on the entire body surface, and consequently condition (2.8) will hold on the extremal surface. Equation (3.15) relates the values of α on the contour of the body base with the Lagrange multiplier ξ_0. The solution of Eq. (3.15) has no effect on the function α, and this means that the value of α^* in condition (2.8) is independent of the given value of S_b.

The value of α^* is such that the surface constructed for $\alpha = \alpha^*$ makes the functional H_0 (3.3) a maximum. The extremum of the functional is sought with $\alpha = \text{const}$, and therefore H_0 may be regarded as a function of the real variables α, defined in the interval [0, 1]: $H_0 = M_0 h(\alpha)$, where

$$h(\alpha) = (h_1(\alpha) + h_2(\alpha))/(\lambda_0\alpha^2)$$
$$h_1(\alpha) = \ln\frac{\lambda_0\alpha^2 + C\gamma/\alpha + 1}{\lambda_1\alpha^2 + C\gamma/\alpha + 1}, \quad h_2(\alpha) = \frac{\ln(\lambda_1\alpha^2 + 1)}{1 + \mu_0\gamma/\alpha}; \quad \lambda_1 = \lambda_1(\alpha) \tag{3.16}$$

If $b \le 0$, where b is defined by formula (1.8), then, independently of α, we have $\lambda_1 = 0$, $h_2(\alpha) = 0$, corresponding to the case of the motion of a body within the limits of model (1.5). In the mixed friction model (1.7), b will satisfy condition (1.8), and if $b/\alpha^2 < \lambda_0$, then $\lambda_1 = b/\alpha^2$, otherwise $\lambda_1 = \lambda_0$. In the latter case $h_1(\alpha) = 0$, and the friction is calculated throughout according to model (1.6).

The maximum of H_0 is sought among the local and boundary extrema of the function $h(\alpha)$. The values of $\alpha = \alpha_m$ at which $h(\alpha)$ attains a local a maximum satisfy the conditions $h'(\alpha_m) = 0$, $h''(\alpha_m) < 0$, and they are found from Eq. (3.14). A boundary maximum of the function $h(\alpha)$ is only possible at $\alpha = 1$. We have $h(1) = ln(1 + \lambda_0)/\lambda_0$, and the local maxima of $h(\alpha)$ must be compared with that quantity. If $h(1) > h(\alpha_m)$, then $\alpha^* = 1$, and the body of maximum penetration depth is an end plane of given area. Consequently, as in the determination of the maximum of $h(\alpha)$ in models (1.5) and (1.6), the quantity α^* is found from condition (3.6), but in the mixed friction model $h(\alpha)$ is defined by formula (3.16). Using the last two relations of (3.13), it can be shown that in the case $h_1(\alpha) = 0$ or $h_2(\alpha) = 0$, corresponding to motion of the body within the limits of models (1.5) or (1.6), Eq. (3.14) takes the form of (3.7).

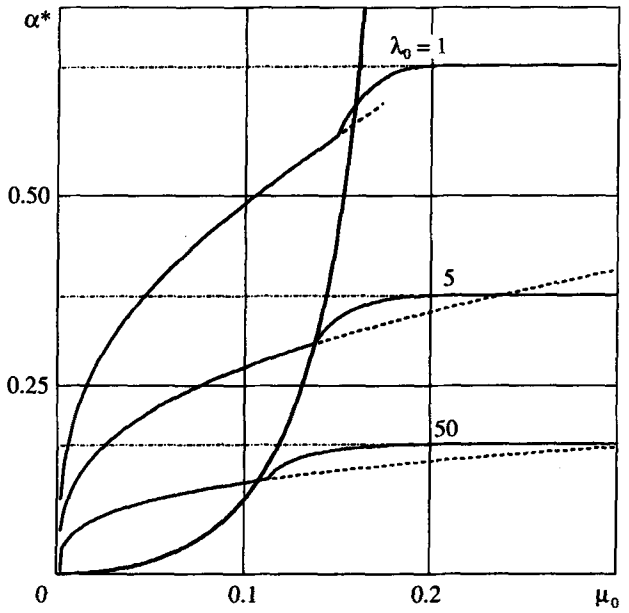

Fig. 4

Solutions of Eq. (3.14) found for $C = 0.2$ are shown as functions of μ_0 in Fig. 4 by solid curves for different λ_0 values. Solutions of Eq. (3.17) found for the same values of C, μ_0 and λ_0 for models (1.5) and (1.6) are shown in Fig. 4 by dot-dash and dashed curves, respectively. It can be seen that for small values of μ_0 the values of α_m obtained from Eq. (3.14) agree with the solutions of Eq. (3.7) found for friction model (1.6), while for $\mu_0 \geq C$ these values agree with the solutions of Eq. (3.7) obtained for friction model (1.5). For fixed C and λ_0, there is a domain of values of μ_0 in which the solutions of Eq. (3.14) differ from those of Eq. (3.7). However, one can see that in that domain the solutions of Eq. (3.14) can be approximated by the values of α_m found from Eq. (3.7) for friction model (1.5). It can be shown that for these μ_0, if $\lambda_0 \in [2, 50]$ and constraints (1.9) hold, the penetration depth for bodies with $\alpha = \alpha_m$, where α_m satisfies Eq. (3.7), will differ from the maximum by less than 2%.

In the mixed friction model (1.7), the Coulomb model (1.6) for the notation of σ_τ is used when condition (2.6) is satisfied, where α_k is evaluated at $\lambda = \lambda_0$. As a result, if the values of α_m found from Eq. (3.14) satisfy condition (2.6) for $\lambda = \lambda_0$, then the friction on the body surface is evaluated over the entire section of the path using model (1.6). In the approximation (2.11), the values of α_m are determined by (3.9), and in that case $E = \mu_0/\lambda_0$. Using formula (3.9), one can find the limiting values of C, λ_0 and μ_0, at which $\alpha_m = \alpha_k$ (2.6). Thus, given C and μ_0, the limiting values of $\lambda_0 = \lambda_k$ are found from the condition

$$\lambda_k = (C/\mu_0 - 1)^3/\mu_0^2 \tag{3.17}$$

and for $C = 0.2$ they are represented as a function of μ_0 by curve 5 in Fig. 2.

As a result, within the limits of the mixed model (1.7) for $\lambda_0 \leq \lambda_k$, a body of maximum penetration depth is constructed for $\alpha = \alpha_m$, where α_m is defined by formula (3.9) with $E = \mu_0/\lambda_0$. The limiting values of $\alpha = \alpha_k$ are also found using the values of C and μ_0: $\alpha_m = \mu_0/(C/\mu_0 - 1)$, and for $C = 0.2$ they are represented by the thickened curve in Fig. 4. This curve, constructed in the approximation (2.11), defines the relation between the limiting values of μ_0 and α_m such that $\alpha_m = \alpha_k$ for $\lambda_0 = \lambda_k$. If $\lambda_0 > \lambda_k$, then $\alpha_m > \alpha_k$, and model (1.6) is more inapplicable. In that case, the s of α_m in approximation (2.11) are approximated by formula (3.9) with $E = C/\lambda_0$. Consequently, in the mixed friction model (1.7) for bodies with maximum penetration depth, as for bodies of minimal drag, approximation (2.15) may be used for α^*, but in that case λ_k will be defined by formula (3.17) and

$$\alpha_1 = (C/\lambda_0)^{1/3}, \quad \alpha_2 = (\mu_0/\lambda_0)^{1/3} \tag{3.18}$$

This approximation, found subject to condition (2.11) and in the framework of the mixed model, is a good approximation of α_m for the local extrema of the function $h(\alpha)$. However, for every λ_0 a B^*

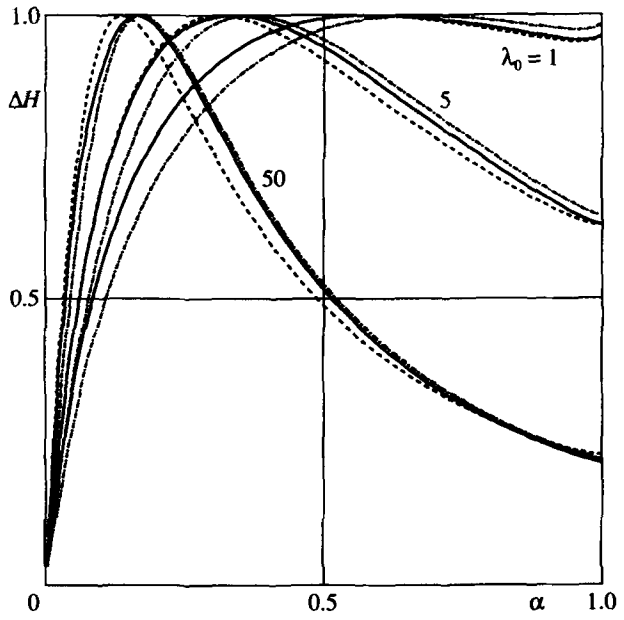

Fig. 5

exists such that, if $B > B^*$, the $\alpha^* = 1$. The values of B^* for friction models (1.5) and (1.6) are given as functions of λ_0 in Fig. 1, and it can be seen that if $\lambda_0 > 2$ and constraints (1.9) holds, then $B < B^*$ for these models. Consequently, for such λ_0, C and μ_0, we have $\alpha^* = \alpha_m$ in friction models (1.5)–(1.7); the approximation (3.9) may be used if models (1.5) and (1.6) are considered, and (2.15) if the mixed model (1.7) is considered, with values of λ_k, α_1 and α_2 taken from formulae (3.17) and (3.18).

The advantages of optimum bodies for penetration depth, compared with other bodies of the same mass and base area, increase together with λ_0. This may be seen by analysing the behaviour of the curves shown in Fig. 5 and representing, for $C = 0.2$ and $\mu_0 = 0.15$, the quotient $\Delta H = H_0(\alpha)/H_0(\alpha^*)$ as a function of α for different values of λ_0. The quantity $H_0(\alpha)$ may be considered in this case as the penetration of cones, constructed for different α, of the same mass and base area as an optimum body. The solid curves in Fig. 5 represent ΔH for the mixed friction model; the dot-dash and dashed curves represent ΔH for friction models (1.5) and (1.6), respectively.

Analysis of the behaviour of the curves in Fig. 5 shows that, for $\lambda_0 = 1$ and $\alpha > 0.3$, the penetration depths of cones differ from the maximum by less than 10%. For $\lambda_0 = 50$ and $\alpha > 0.3$, the differences already exceed 20%; for example, the penetration depth of an optimum body exceeds that of a cylinder of the same mass and base area, with $\alpha = 1$ on its leading face, by a factor of almost 5.

Our result – the weak dependence of the penetration depth on the body shape when $\lambda_0 \sim 1$ – agrees with the conclusion drawn in [16] from an analysis of experimental data on the penetration depth of ogival bodies in concrete. It was shown in [16] that up to a velocity $U_0 = 460$ m/s the penetration depth of the bodies is well approximated by formulae obtained on the assumption that the dynamic component in formula (1.2) for σ_n (1.2) is small compared with the strength component. Note that the velocity $U_0 = 460$ m/s for concrete corresponds to $\lambda_0 \approx 2$.

Analysis of a large body of experimental and theoretical data relating to the penetration depth of bodies of various geometries in such media as soil, concrete, and metal implies that, up to penetration velocities U_0 corresponding to $\lambda_0 \approx 5$, there is little difference between the depths to which different bodies penetrate [10]. It has been conjectured that at such velocities the problem of optimizing the body shape is not of the essence, since under those conditions the differences between penetration depths of bodies of different geometries amount to at most 10–15% [10]. One can agree with this last conclusion only provided the bodies considered vary over a limited range of relative thicknesses. For $\lambda_0 \leq 5$, the function $H_0(\alpha)$ does not have a sharply expressed maximum; in that case, therefore, it is quite possible that the penetration depths of different bodies will differ only slightly. Outside that range of thicknesses, however, the differences may increase. Analysis of the behaviour of the curves constructed in Fig. 5 for $\lambda_0 = 5$ shows that when $\alpha > 0.4$, an increase in the relative thickness of a cone leads to a loss of penetration depth in the optimal body; for a body with $\alpha = 1$ this loss may reach as much as 60%.

Thus, within the framework of the two-term local interaction model (1.2), using friction models (1.5)–(1.7), we have compared the solutions of the problem of the shape of a body with maximum penetration depth. It has been shown that, for a given mass and base area of the body, in all the friction models, the optimum shape is constructed subject to the condition (2.8), where α^* is determined by the parameters λ_0, C and μ_0. If $\lambda_2 \geq 2$, then $\alpha^* = \alpha_m$ and the value of α^* is approximated by formula (3.9) if the friction model considered is (1.5) or (1.6), or by formula (2.15) with values of λ_0, α_1 and α_2 taken from formulae (3.17) and (3.18) if the mixed model (1.7) is considered. If $\lambda_0 \in [2, 50]$ and constraints (1.9) hold, these approximations enable bodies to be constructed whose penetration depth deviates from the maximum by less than 2%.

In conclusion, it should be mentioned that the values $\lambda_0 \in [2, 50]$ for which approximations and estimates have been obtained in this paper include the most interesting range of initial velocities of bodies moving in different media, from a practical point of view. As the velocity λ_0 increases, the advantages of optimum bodies are enhanced as regards lower drag and deeper penetration compared with other bodies. However, there is always a value λ^* such that when $\lambda_0 > \lambda^*$ the penetrating body is deformed. Optimization problems for bodies are solved on the assumption that the shape of the body is not distorted during motion, and the solutions of these problems are meaningful only when $\lambda_0 \leq \lambda^*$. The actual value of λ^* depends on the properties of the medium and the strength characteristics of the material of the impactor. Analysis of experimental data for a steel projectile penetrating concrete [15] and aluminium [17] shows that in these media deformation of a steel projectile begins at a velocity $U_0 = U^*$, $U^* \approx 1500$ m/s, which corresponds to $\lambda^* \approx 20$ for concrete and $\lambda^* \approx 5$ for aluminium. No similar experiments have been published for soil, but we may assume that, since the friction forces in soil are higher than in metal, the velocity U^* should be lower. In low and medium strength soils, a value of $\lambda_0 = 50$ corresponds to $U_0 \approx 700$ to 1000 m/s and these velocities may be considered to be the limiting ones for soils as long as the projectile has not yet been deformed.

This research was supported financially by the Russian Foundation for Basic Research (04-01-00771) and the "State Support for the Leading Scientific Schools" programme (NSh-2124.2003.1).

REFERENCES

1. GRIGORYAN, S. S., A new friction law and the mechanism of large-scale avalanches and landslides. *Dokl. Akad. Nauk SSSR*, 1979, **244**, 4, 846–849.
2. ZUKAS, J. A., NICHOLAS, T., SWIFT, H. F., *et al.*, *Impact Dynamics*. Wiley, New York, 1982.
3. CHEN, E. P., Penetration into dry motion porous rock: a numerical study on sliding friction simulation. *Theor. Appl. Fract. Mech.*, 1989, **11**, 135–141.
4. MIELE, A. (Ed), *Theory of Optimum Aerodynamic Shapes*. Academic Press, New York, 1965.
5. FLITMAN, L. M., Subsonic axisymmtric elasto-plastic flow around thin sharp solid of revolution. *Iav. Akad. nauk SSSR, MTT*, 1991, 4, 153–164.
6. FOMIN, V. M., GULIDOV, A. I., SAPOZHNIKOV, G. A., *et al.*, *High Velocity Interaction of Bodies*. Izd. Sibirsk. Otd. Ross. Akad. Nauk, Novosibirsk, 1999.
7. JONES, S. E. and RULE, W. K., On the optimal nose geometry for a rigid penetrator, including the effect of pressure-dependent friction. *Intern. J. Impact Engng*, 2000, **24**, 403–415.
8. YAKUNINA, G. Ye., Three-dimensional shapes of a body with maximum penetration depth in dense media. *Dokl Ross. Akad. Nauk*, 2001, **376**, 6, 768–771.
9. OSTAPENKO, N. A., Solids of revolution of minimum drag moving in dense media. *Uspekhi Mekhaniki*, 2002, **1**, 2, 105–149.
10. CHEN, X. W. and LI, Q. M., Deep penetration of a non-deformable projectile with different geometrical characteristics. *Intern. J. Impact Engng.* 2002, **27**, 619–637.
11. YAKUNINA, G. Ye., Effects of sliding friction on the optimal 3D-nose geometry of rigid rods penetrating media. *J. Optimiz. and Engng.* 2005, **6**, 3, 315–338.
12. YAKUNINA, G. Ye., Optimal non-conical and non-symmetric three-dimensional configurations. *Prikl. Mat. Mekh.*, 2002, **64**, 4, 605–614. *Gas Dyamics. A Selection*, Vol. 1 (Edited by A. N. Kraiko). Fizmatlit, Moscow, 2000, 431–442.
13. KRAIKO, A. N., PUDOVIKOV, D. Ye. and YAKUNINA, G. Ye., *The Theory of Close to Optimal Aerodynamic Shapes*. Yans-K, Moscow, 2001.
14. YAKUNINA, G. Ye., Three-dimensional bodies of minimum total drag in hypersonic flow. *J. Optimiz. Theory and Appl.*, 2002, **115**, 2, 241–265.
15. FREW, D. J., FORRESTAL, M. J. and HANCHAK, S. J., Penetration experiments with limestone targets and ogival-nose steel projectiles. *Trans ASME. J. Appl. Mech.*, 2002, 67, 841–845.
16. FORRESTAL, M. J., FREW, D. J., HICKERON, J. P. and ROHWER, T. A., Penetration of concrete target with decelaration-time measurements. *Intern. J. Impact. Engng*, 2003, **28**, 479–497.
17. PIEKUTOWSKY, A. J., FORRESTAL, M. J., POORMON, K. L. and WARREN, T. L., Penetration of 6061–T651 aluminum targets by ogival-nose projectiles with striking velocities between 0.5 and 3.0 km/s. *Intern. J. Impact Engng.* 1999, **23**, 723–734.

Translated by D.L.